Effects of noise on the turn-on dynamics of a modulated class-B laser in the generalized multistability domain

S. I. Turovets,[1,*] A. Valle,[2] and K. A. Shore[1]

[1]*University of Wales, Bangor, School of Electronic Engineering and Computer Systems, Bangor LL57 1UT, Wales, United Kingdom*
[2]*Instituto de Fisica de Cantabria, CSIC-UC, E39005 Santander, Spain*

We have investigated the influence of intrinsic laser noise on recently proposed schemes for targeting laser dynamics to unstable periodic orbits by means of Q switching of modulated class-B lasers. Several interesting features of turn-on statistics in such a nonlinear regime have been found, including scaling of targeting peaks location with the strength of the spontaneous emission noise and universality of the transient time statistics, i.e., their essential independence of the strength of noise. The concept of the highest passage times has been introduced and their distribution functions double-peaked structure with the underlying symmetry properties has been revealed and explained. The noise has been found to cause much more frequent phase switching in comparison with the deterministic case with possible detrimental effects on the use of this particular scheme in chaos control techniques. [S1050-2947(97)09003-3]

PACS number(s): 42.55.−f

I. INTRODUCTION

Transient statistics of a laser switch-on have been a subject of intense studies since the advent of the laser [1]. From a fundamental point of view such investigations give insight into the basic processes triggered by quantum noise in macroscopic nonequilibrium systems. In applications, the turn-on delay jitter caused by spontaneous emission plays a significant role in determining optical communication system performance, and has been investigated both experimentally [2], using numerical simulations [3] and also analytical methods [4]. However, the results reported so far in literature (see, e.g., the review by San Miguel [4] of the situation in the field) have dealt mainly with dynamics only near the lasing threshold, or from the point of view of the general dynamical system theory, the first laser instability, whereas in the laser, as a typical nonlinear dynamical system, the full hierarchy of instabilities, including different bifurcating routes to chaos, have been found to exist [5]. For a bifurcating laser the phase space is more complicated, and a trajectory may pass near one of the unstable orbits during the course of relaxation from the nonlasing unstable state and thus significant modification of turn-on statistics might be anticipated. In an earlier paper [6], using fully deterministic numerical simulations of a Q-switched class-B laser with modulated losses or a saturable absorber, the possibility of steering dynamics to unstable lasing states during transient processes has been shown. Nonetheless, transient statistics of laser dynamics from the off-state to one of the attractors in the generalized multistability domain or the period-doubling regime have not yet been studied theoretically in any detail. That is the aim of the present paper.

The classification of lasers A, B, and C was introduced in Ref. [7] and is based on relations between cavity and active

material relaxation times. For class-B lasers, the dephasing time of the active material dipole moment is much shorter than both the cavity photon lifetime and the population inversion decay time, so that the polarization of the active medium adiabatically follows the cavity field and may be eliminated from consideration. Most solid-state lasers, semiconductor lasers, and certain molecular lasers (e.g., CO_2) belong to this class. The general property of class-B lasers distinguishing them from class-A lasers (He-Ne, Ar, dye) is that they readily exhibit relaxation oscillations lending themselves for modulation. This is why under moderate strength of modulation the dynamical response of such lasers becomes strongly nonlinear, and the lasers display a rich variety of nonlinear phenomena, ranging from bistability to the period-doubling route to chaos, as has been shown in great detail both theoretically and experimentally (see, e.g., [8] and references therein). In what follows, we consider Q switchings of a single mode class-B laser with sinusoidally modulated cavity losses with a control parameter set just above the first period-doubling bifurcation taking into account intrinsic noise. As only intensity transient statistics are of interest, no explicit treatment of the phase of the laser field is required here.

II. MODEL

The effects of spontaneous emission and pump noises on the class-B laser dynamics can be well described in the framework of the Langevin formulation of the coupled cavity and atomic rate equations for the number of photons n and inversion population $N = N_2 - N_1$ of the lasing pair of levels [9]

$$dn/dt = (KN - \gamma_c(t))n + R_{sp} + F_n(t), \tag{1}$$

$$dN/dt = r_p - \eta KNn - \gamma_2 N + R_N(t), \tag{2}$$

where K is the field-matter coupling constant, r_p is the pumping rate, and γ_2 is the population decay rate. The pa-

*On leave from Institute of Physics, Academy of Sciences, 70 Skarina Avenue, Minsk 220072, Belarus.

rameter η accounts for two possible modification of the rate equations: in the case of a two-level system, with a fixed total population ($N_2+N_1=N_0$), $\eta=2$; in the case of a four-level system (with the lower-level depopulation rate being sufficiently fast so that $N_1\cong0$ and $N\cong N_2$ under all circumstances) $\eta=1$. The photon cavity decay rate is taken in the form $\gamma_c(t)=\gamma_c^{(2)}(k(t)+m\,\cos(\omega_m t+\varphi))$, where m, ω_g, and φ are the modulation depth, frequency, and arbitrary phase, and $k(t)$ accounts for sudden Q switching at the moment of time $t=0$, being equal to the hold-off ratio $k=\gamma_c^{(1)}/\gamma_c^{(2)}>1$ for $t<0$, and 1 otherwise. The influence of spontaneous emission is taken into account by the average rate term

$$R_{sp}=\beta\gamma_{rad}N_2, \tag{3}$$

which yields the mean power spontaneously emitted into the lasing mode, and the corresponding Langevin force, which describes the fluctuations of this mean power:

$$F_n(t)=(2R_{sP}n)^{1/2}\xi(t)$$

with

$$\langle\xi(t)\xi(s)\rangle=\delta(t-s)\ \ \text{and}\ \ \langle\xi(t)\rangle=0, \tag{4}$$

where γ_{rad} is the radiative decay rate from the upper level, and β is the spontaneous emission factor specifying the fraction of the total spontaneous emission, which is coupled to an individual cavity mode. In the population equation the stochastic term

$$R_N(t)=(R)^{1/2}\ \zeta(t)$$

with

$$\langle\zeta(t)\zeta(s)\rangle=\delta(t-s)\ \ \ \text{and}\ \ \ \langle\zeta(t)\rangle=0 \tag{5}$$

accounts for several different sources (e.g., density and temperature fluctuations in an active medium which are usually dominant over quantum shot noise) and which will be treated phenomenologically when required. The zero-mean Gaussian noises $\xi(t)$ and $\zeta(t)$ are assumed to be mutually uncorrelated. Having rescaled variables as follows—$y=N/N_{trh}=KN/\gamma_c^{(2)}$, $u=n/n_{sat}=\eta Kn/\gamma_2$, $\tau=\gamma_2 t$—and assuming for simplicity $\gamma_{rad}=\gamma_2$, it is possible to reduce Eqs. (1) and (2) to the dimensionless forms

$$du/d\tau=\nu(y-k(\tau)=m\,\cos(\omega\tau+\varphi))u+r_{sp}$$
$$+(2r_{sp}u)^{1/2}\xi(t), \tag{6}$$

$$dy/d\tau=y_0-(1+u)y+(\delta)^{1/2}\zeta(t), \tag{7}$$

where our parameters are given by $\nu=\gamma_c^{(2)}/\gamma_2$, $y_0=Kr_p/(\gamma_c^{(2)}\gamma_2)$, $\omega=\omega_m/\gamma_2$, $\delta=(R/\gamma_2)K^2/(\gamma_c^{(2)})$, and $r_{sp}=\nu\beta y$ in the case of a four-level system with a fast lower lasing level, and $r_{sp}=\nu\beta(y+KN_0/\gamma_0^{(2)})$ in the case of a two-level system with a fixed total population N_0.

It can be seen that the normalized equations contain fewer parameters than the original ones. This gives relative freedom in referring the results obtained to specific lasers. The dimensionless form of the rate equations is useful also in another respect: the model (1)–(2) is, in general, too ideal-

ized to describe the dynamics of a specific laser quantitatively; nevertheless, it gives a fairly good approximation in many cases when the dimensionless parameters have been chosen to match experimental results, e.g., relaxation oscillation frequency and their decay times. The parameter β may be estimated by fitting an experimental laser output-pump characteristic to the steady-state solution of Eqs. (6) and (7) for the unmodulated case ($m=0$) with $\eta=1$ and constant cavity losses k,

$$u_{st}=[y_0-k+((y_0-k)^2+4k\beta y_0)^{1/2}]/2k. \tag{8}$$

In the following, unless otherwise stated, we do not restrict ourselves to any specific choice of laser parameters (in particular β, which may be varied from 10^{-10} for bulk lasers up to nearly 1 for the recently developed microcavity semiconductor lasers) but rather, using the given dimensionless parameters, we illustrate the general tendency in nonlinear dynamics as the noise strength progressively increases. Finally, we observe that the simplest model of a laser diode (without taking into account gain saturation effects, the linewidth enhancement factor, etc.) is isomorphic to Eqs. (6) and (7), so the results obtained in this consideration may be applicable to their dynamics as well.

III. RESULTS

In all calculations reported below we have chosen parameters $y_0=2$ and $\nu=70$, which reflects a common case for class-B lasers, when the laser is assumed to be pumped at twice threshold and only a few spikes are observed in relaxation oscillations toward a steady state. The modulation strength is assumed to have been set to the value that ensures the period-doubling regime. A quite accurate estimate for the lower threshold of a period-doubling bifurcation in the system at $\omega\cong2\omega_{rel}=2(v(y_0-1))^{1/2}$ can be obtained from a Floquet stability analysis [10] yielding $m_{th}\cong3y_0/\nu$ for $r_{sp}=0$. For $y_0=2$, $\nu=70$ this gives $m_{th}\cong\frac{6}{70}$. In the present calculations we have fixed the modulation depth comfortably above this threshold taking $m=0.1>\frac{6}{70}$, and varying ω slightly around $2\omega_{rel}$. The hold-off ratio k is taken to be 4, so for a small β and $\eta=1$ Eq. (8) gives the stationary laser intensity before Q switching $u_{st}\cong\beta$, and $y_{st}\cong2(1-\beta)$. For the nonmodulated case it is easily checked that below threshold the stochastic equation for the laser field can be treated as a linear complex Ornstein-Ulenbeck process yielding the exponential probability density distribution for intensity in a steady state: $P_u=\langle u\rangle^{-1}\exp(-u/\langle u\rangle)$ with a second moment $\langle u^2\rangle-\langle u\rangle^2=\langle u\rangle^2$ [11]. Furthermore, it is found, using standard techniques [12], that in the small-signal modulation regime considered here the exponential distribution is maintained (albeit with a slight change in the average value). An event of laser Q switching is modeled by numerical solution of the stochastic Eqs. (6) and (7) with the deterministic initial conditions $u(\tau\leqslant0)=\beta$, $y(\tau\leqslant0)=2(1-\beta)$, which correspond to the average number of spontaneous photons and population inversion in the laser off-state. Thus, at the moment of Q switching, $\tau=0$, there already exist ``randomized'' variables u and y with corresponding rms deviations β and 2β. So the actual build-up laser intensity is initialized
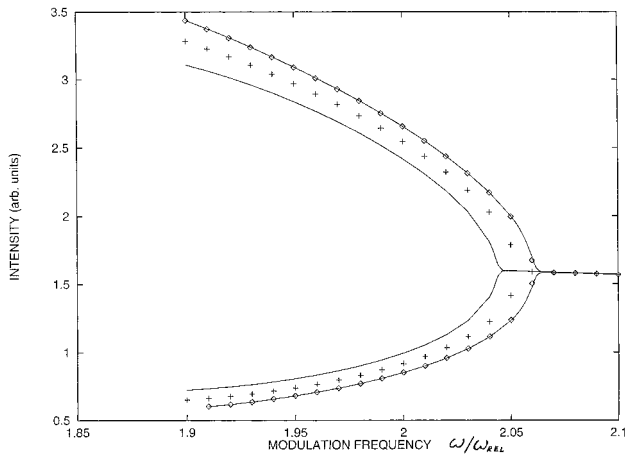
FIG. 1. First period-doubling bifurcation diagram for spontane-
ous emission factor $\beta=0$ (—, right), 10^{-4} ($\diamond$), 5×10^{-4}
(+), 10^{-3} (—, left), $\nu=70$, $y_0=2$, and $m=0.1$.

from the noisy cloud centered at the stationary point, and of
a radius of approximately β.

Inasmuch as the initial conditions have been chosen near
their average values in the nonlasing regime, the duration of
the ''thermalization'' stage is quite short and may be taken
as a few periods of modulation. It should be pointed out that
in the deterministic simulations $(r_{sp}=0)du/d\tau=0$, when-
ever $u(0)=0$, therefore lasing is not possible without some
initial seeding. The influence of a nonzero spontaneous emis-
sion term $r_{sp}=\nu\beta y$ is known to be capable of shifting the
whole bifurcation diagram slightly to higher values of the
modulation index, primarily due to the extra damping of re-
laxation oscillations and making the laser Toda potential
more symmetrical [13]. In Fig. 1 we present the results of
numerical calculations of such influence on the period-
doubling bifurcation for the parameter domain of interest. It
is seen that the bifurcation is supercritical and almost insen-
sitive to the spontaneous contribution up to $\beta\cong10^{-4}$; after-
wards the effect of the shrinking of the instability starts to
increase quickly with β. The latter fact explains, for in-
stance, why laser diodes (having $\beta\cong10^{-4}-10^{-5}$) normally
exhibit only a few period-doubling bifurcations even under
strong modulation.

A. Deterministic case

Poincaré section. The dynamical evolution of the laser as
prescribed by Eqs. (1) and (2) [or in normalized form in Eqs.
(6) and (7)] occurs in a three-dimensional phase space whose
coordinates are defined by the photon number, the inversion,
and time. The dynamics of the system can then be seen as
trajectories along the time axis. Understanding of complex
dynamics in such systems is aided considerably by perform-
ing a periodical sampling of the phase-space dynamics. In
this way a stroboscopic projection of the dynamics onto a
two-dimensional plane known as a Poincaré section or Poin-
caré map is obtained [14]. Such a procedure has been applied
here in the vicinity of the first period-doubling bifurcation of
the laser dynamics. Poincaré sections are readily obtained
using standard numerical techniques [14]. In Fig. 2, the Poin-
caré section for the deterministic case ($\beta=0$) was obtained
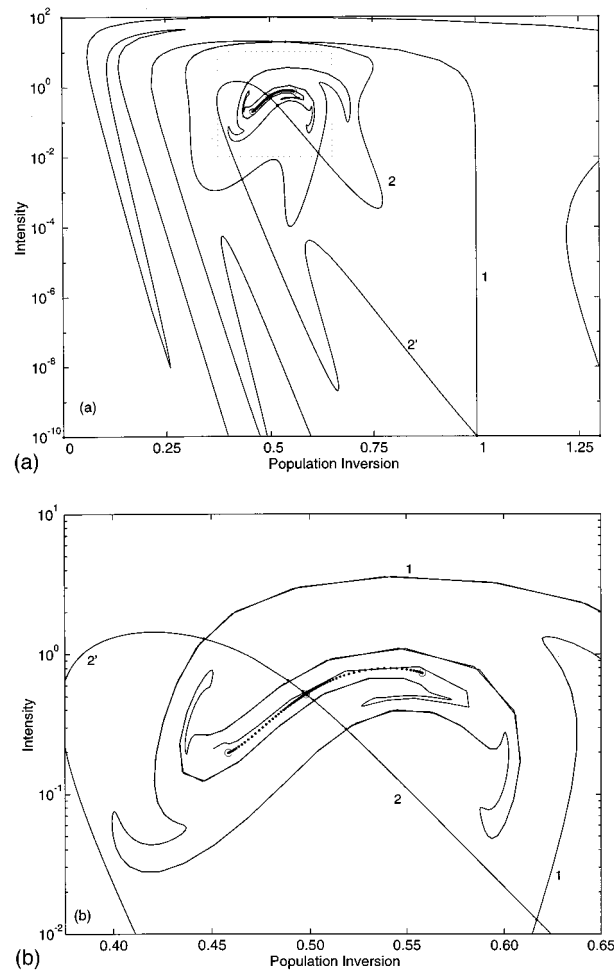
FIG. 2. (a) The Poincaré section of the modulated laser system
prepared just after the first period-doubling bifurcation in the deter-
ministic case ($\beta=0$) for $\varphi=0.4\pi$, $\omega/(\nu(y_0-1))^{1/2}=1.9$. The
other parameters are as in Fig. 1. Curve 1 is the outset of nonlasing
steady state ($u=0$, $y=y_0$). Curves 2 and $2'$ are the insets of the
unstable T-periodic cycle. The thick line corresponds to the outsets
of the unstable T-periodic cycle terminating at two stable $2T$ cycle
[see also (b)]. The intersection points of curve 1 and curves 2 and
$2'$ are shown by the small black circles, and correspond to the
actual turn-on trajectory with the initial conditions
$[u(0)=10^{-10}$, $y(0)=y_0]$ during the course of the targeting pro-
cess. (b) Expanded version of (a). The dotted line corresponds to
the outset of the T-periodic cycle terminating at two stable $2T$
cycles [the thick line in (a)].

by sampling at the modulation frequency starting from
$\tau=0$ with the modulator phase φ fixed at 0.4π.

The stable and unstable fixed points of the Poincaré map
may be found as the points minimizing the distance between
the input point and its Poincaré image. (The fixed point cor-
responding to the nonlasing steady state is found immedi-
ately, for $\beta=0$, as $u=0$ and $y=y_0$.) The stable fixed points
can, in fact, be found directly as the attractors of the system.
The identification of the unstable fixed points is aided in the
present work by the targeting method which is described
below. The initial modulation phase at the Q-switching event
can be tuned so that the system arrives directly at the re-
quired unstable fixed point and remains there for a relatively
long period of time. In practice a rather simple ''trial and

error'' method based on this procedure was successfully applied in this work. Then stable and unstable manifolds are calculated by taking sets of initial conditions along the eigendirections of the linearized map near the unstable fixed point, and propagating these sets backward and forward in time. In the case of a nonlasing fixed point it is reasonable to choose this initial set of points as being uniformly distributed over the so-called T segment of the unstable manifold. Here the T segment is defined as a segment of the manifold whose ends are the sequential iterates of the Poincaré map, i.e., they are mapped into each other at every modulation period T. Use is also made below of the terms ''insets'' and ''outsets'' which, as defined in [14], refer to trajectories which are asymptotic to a saddle point: the insets are asymptotic as $\tau \rightarrow \infty$ and the outsets are asymptotic as $\tau \rightarrow -\infty$. Insets (outsets) correspond to incoming (outgoing) eigenvectors with negative (positive) eigenvalues.

The key elements of the Poincaré section under consideration are the unstable saddle T-periodic orbit ($T = 2\pi / \omega$) and its insets Fig. 2(a) (curves 2 and 2′) which are infinitely spiraling out backward in time forming a ''swan's head.'' The insets serve as separatrixes and determine which of the two antiphased $2T$-periodic attractors will be reached starting from the given initial conditions. Figure 2(a) also depicts the outset of the nonlasing saddle point (curve 1) and the outsets of the unstable saddle T-periodic orbit which terminate at the only $2T$-periodic attractors in this setting [the thick line in Fig. 2(a) which is shown as the dotted line in the expanded Fig. 2(b)]. When the stroboscopic view is taken at a different time (or, equivalently, modulator phase), the whole picture (except the nonlasing state and its manifolds) rotates in the (u,y) frame. In Fig. 2 the phase of modulator has been deliberately chosen to make the separatrix 2′ pass through the assumed initial point ($u = 10^{-10}$ and $y = y_0$). In this case the system is ''confused:'' it must follow the outset of the nonlasing steady state (curve 1), and, on the other hand, the inset 2′ which leads eventually to the unstable orbit. A compromise in fact is readily available, taking into account the stroboscopic nature of the Poincaré section: an actual trajectory of laser turn-on follows all the points of intersection of curves 2, 2′, and 1 [the sequential iterates are marked by small black circles in Fig. 2(a)] and passes through the unstable T-periodic orbit.

Generally, the dynamics of the bifurcating system is determined by the presence of the unstable orbits and the behavior of their invariant manifolds. This behavior is governed by simple rules which are based on the fundamental theorem of existence and uniqueness of the solution of an ordinary differential equation under given initial conditions. In particular, only manifolds belonging to different saddle points which are opposite in respect of stability are allowed to intersect each other transversally in our heteroclinic setting. In our case, for instance, intersections of curve 1 and curves 2 and 2′ are allowed, but intersections of curve 1 with the outset of the T-periodic cycle [the thick line in Fig. 2(a) and the dotted line in the expanded Fig. 2(b)] are prohibited. As a consequence, curves 2 and 2′ intersect the outset of the nonlasing state an infinite number of times as $\tau \rightarrow -\infty$, approaching its stable manifold tangentially and forming a densely packed heteroclinic structure. In turn, the outset of the nonlasing state (curve 1) behaves similarly—spiraling

down to the unstable manifold of the T-periodic cycle and approaching it tangentially as $\tau \rightarrow +\infty$.

In Fig. 2 the simplest nondegenerate case of mutual behavior of the separatrix and the outset of the nonlasing state is shown, when only one intersection at the T-segment takes place ($\omega = 1.9 \omega_{\mathrm{rel}}$). Here, as noted above, the T segment means a segment of the manifold (curve 1) whose ends are mapped into each other in the modulation period T. In the general case, due to the additional separatrix foldings in the vicinity of the bifurcation point, the intersections at the T segment are multiple. In the particular case of degeneracy, the additional folding just touches curve 1 tangentially. The specific pattern of the behavior of the manifolds in the Poincaré section is completely defined by the number and type of attractors and repellers in the system for the given parameters. It has been shown through a systematic study of the parameter range where these patterns take place [6] that the simplest picture (only one intersection) is observed almost exactly at double the nonlinear resonance: $\omega / \{v(y_0 - 1)\}^{1/2} = 1.9$. As the modulation frequency is detuned and approaches the inverse period-doubling bifurcation point [cf. Fig. 1: $\{\omega / v(y_0 - 1)\}^{1/2} = 2.07$] the picture is complicated due to extra intersections arising in pairs with additional foldings—up to five crossings were found in [6]. It may further be speculated that the number of intersection points approaches infinity as the control parameter approaches the bifurcation point. The basis of such a conjecture is the observation that close to the bifurcation point two $2T$-periodic attractors and the unstable T-periodic orbit are about to emerge. As such, it can be anticipated that a tiny inaccuracy in initial conditions can lead to different period-2 orbits—a condition which could be possible only in the case where the separatrix experiences more foldings near the bifurcation point. The proof of this conjecture represents a challenging mathematical problem. Alternatively confirmation of the conjecture can be sought via numerical simulations. It is noted, however, that due to the effects of critical slowing down near the bifurcation point this would require rather extensive computations. As such, it is not possible to indicate *a priori* precisely how many separatrix foldings occur for arbitrary parameter values.

Targeting the unstable T-periodic orbit. The special values of the modulator phase when the laser goes through the unstable T-periodic orbit during the course of the transient can be called the targeting phases, and might be considered as a way of preparing the system in the unstable state before applying one of the recently developed schemes of feedback-monitored control [15]. In the deterministic situation the relaxation time (the duration of the transient) diverges at the targeting phases, because in the absence of noise the system might become trapped in the unstable orbit for quite a long time, notwithstanding inevitable numerical noise. The total number of such phase values in the interval $[0, 2\pi]$ is odd in the nondegenerate case and depends on the location of the control parameter relative to the period-doubling bifurcation boundaries. In practice the phase values are easy to find by continuously sweeping the modulator phase over an interval 2π and looking at the relaxation time to the final $2T$-periodic attractors. Obviously, such dependencies of the relaxation time versus modulator phase should reveal a structure consisting of sharp peaks at the targeting phases and
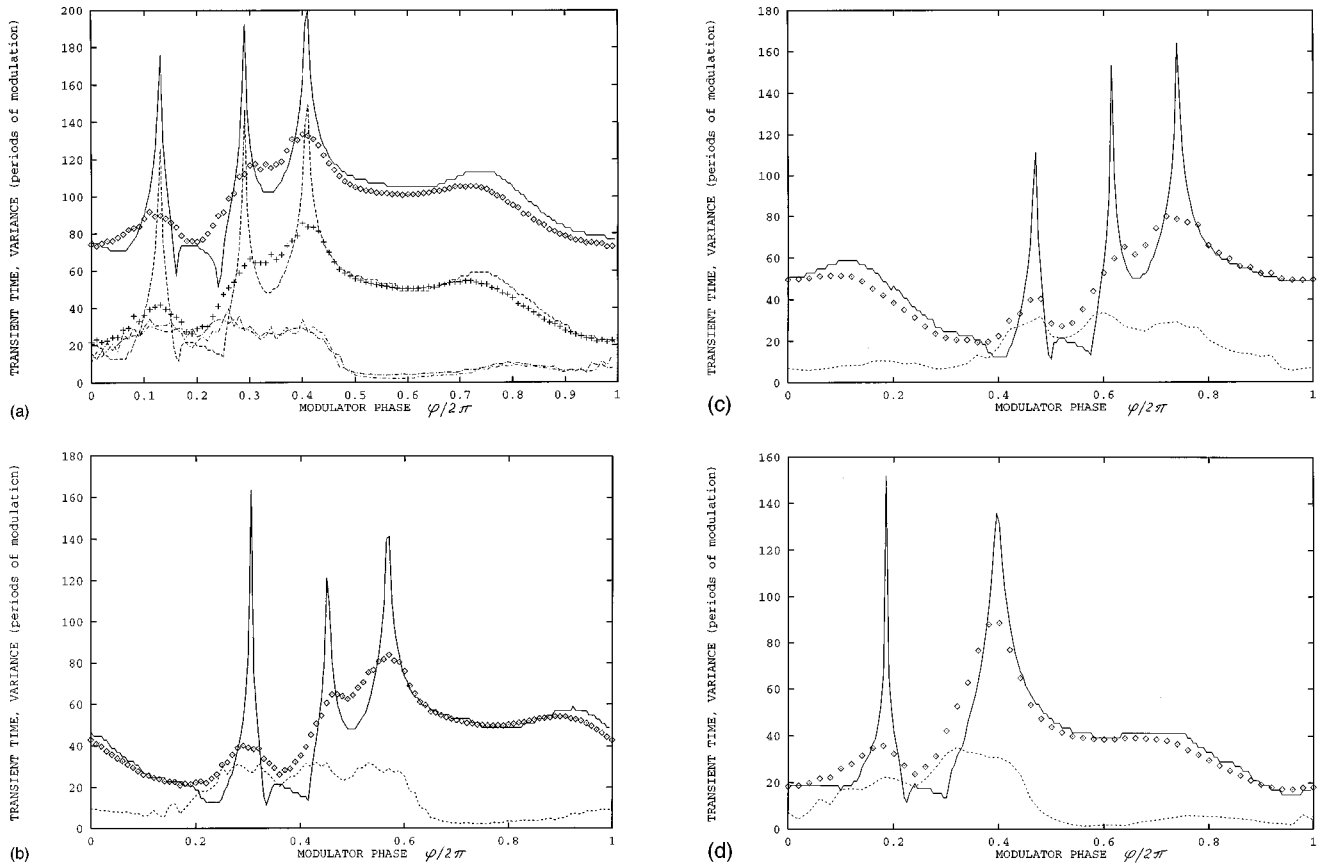
FIG. 3. The transient time vs the modulator phase: deterministic case (no Langevin noise) (solid lines), spontaneous Langevin term included (points); variance of the transient time: (a) dash-dotted, (b)–(d) dashed curves. Spontaneous emission factor: $\beta = 10^{-10}$ (a) and (d), 10^{-8} (b), 10^{-6} (c); $\omega/(\nu(y_0-1))^{1/2} = 2$ (a)–(c), and 1.95 (d). Other parameters are as in Fig. 1. The bottom and top plots in (a) are taken with the criterion for T_{tr} to be 0.1 and 0.0001, correspondingly.

broadened peaks in degeneracy, when the separatrix folding just approaches the initial point tangentially.

Examples of such patterns are presented in Figs. 3(a)–3(d) by solid lines for different spontaneous deterministic terms and modulation frequencies. The transient time T_{tr} has been defined as the time of settling down to the final $2T$-period regime with a prescribed accuracy. This means that the integration was performed until the envelope of the $2T$-periodic solution was conserved with this accuracy. More precisely, use was first of all made of the criteria $|u(\tau)-u(\tau-2T)|/u(\tau) < 10^{-4}$, $|u(\tau)-u(\tau-T)|/u(\tau) \geqslant 10^{-4}$, where τ is when the maximum of u appears [Fig. 3(a), top dependencies]. The second inequality guarantees that the integration does not stop at targeting values of phase, when the long-lived patterns of T-periodic regimes might be observed in transients. However, it is obvious that such a criterion cannot be universal as soon as noise is included in the calculations, because then the laser output fluctuates even in the steady state, albeit much less than during the transients. For the noise strengths used in this paper (up to $\beta \cong 10^{-4}$) we have found that using a tolerance of 10^{-1} in the criteria to be quite adequate in all circumstances. As can be seen from comparison of the top and the bottom dependencies in Fig. 3(a), which are calculated with these two different criteria (here $\beta = 10^{-10}$), some subtle details like narrow dips are lost in this way. However, the main consequence of relaxing the criteria is merely to cause a global

downward shift of all the curves. The narrow dips themselves corresponds to the fast manifolds of the $2T$-periodic attractors, and are not related directly to the targeting phases. At this point it is noted that deterministic calculations with high resolution in phase give ''fingerprints'' of all the important geometrical features of the Poincaré section, including the number and kind of unstable orbits and anisotropy of the phase space (in terms of the fast and slow manifolds), and may be used as an alternative tool in exploring the nonlinear dynamics of similar systems.

The heights of deterministic peaks at the targeting phases are in principle infinite: in Figs. 3(a)–3(d) their heights are limited simply by the finite resolution in phase—taken to be 0.01π. In Figs. 3(a)–3(c) the modulation frequency $\omega = 2\omega_{\mathrm{rel}}$ allows three peaks to be observed. Two peaks at the right side merge into one at $\omega = 1.95\omega_{\mathrm{rel}}$ (degenerate case), as shown in Fig. 3(d). Upon further reduction of the modulation frequency this peak is broadened, and evolves into one with a finite amplitude corresponding to the vicinity of the separatrix folding. The most striking feature of these dependencies is their self-similarity for different averaged spontaneous contribution (under otherwise identical conditions), as can be seen from comparison of Figs. 3(a)–3(c). To illustrate this point in more detail, we have plotted the phase of the maxima's positions as a function of $\log_{10}\beta$ in Fig. 4. It can be seen that in a huge range of β all three peaks move almost linearly with $\log_{10}\beta$, and the distances between them
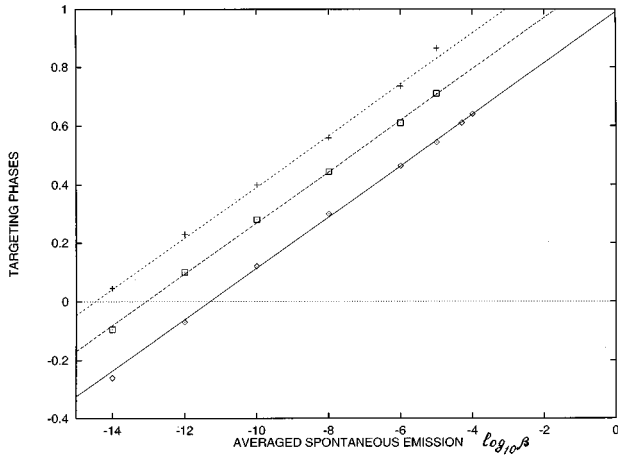
FIG. 4. The targeting phases [maximum in Figs. 3(a)–3(c)] vs the spontaneous factor β on a decimal semilogarithmic scale. The straight lines are the best fits of the analytical estimate [Eq. (11)] to the numerical data.

also being conserved. This indicates some common underlying mechanism.

The explanation of this linear law is essentially based on the linear theory of relaxation from the nonlasing point and signifies little more than the dependence of the timing (or phase) on the initial intensity for lasing which is itself proportional to β. Indeed, to reach the targeting regime we may either vary the phase for the given initial conditions or, alternatively, change the initial intensity for fixed phase (cf. Fig. 2) varying β or k and advancing along the unstable manifold of the off-state to the next point of intersection with the stable manifold of the unstable T-periodic fixed point. In the linear regime ($u \lesssim 0.1$) the increase in the initial intensity $u(0)[u(0) = \beta y_0 / (k - y_0)]$ is prescribed via

$$u(T) = u(0) \exp(\gamma T), \qquad (9)$$

where $\gamma = v(y_0 - 1)$ is the net gain over the modulation period T. On the other hand, the targeting phases which differ by 2π correspond to successive intersections of curve 1 with curves 2 and 2′, and are ends of the T segment whose intensities are also given via Eq. (9). Thus the 2π change in phase is equivalent to a change of initial intensity by the factor $\exp(\gamma T)$. Therefore it is possible to write the map

$$u_2(0) = u_1(0) e^{\gamma T}, \quad \varphi_2 = \varphi_1 + 1, \qquad (10)$$

where the phase is normalized to 2π. Assuming the linear dependence

$$\varphi_{\max} = A \, \log_{10}(\beta y_0 / (k - y_0)) + B, \qquad (11)$$

we obtain

$$A = \omega / (2\pi \log_{10}(e) \nu (y_0 - 1)), \qquad (12)$$

which fits very well to the observed linear law ($k = 4$) in Fig. 4 (the lines are the best fits of the analytical linear dependence to the data shown by points with $B \sim 1$). More detailed calculations will be presented elsewhere [16] to take into account T-periodical oscillations of the outset 1 with chang-

ing φ and more accurate calculations of the eigenvalues and eigenvectors of the laser off-state.

B. Stochastic case

Spontaneous noise and universality of statistics. In this section we describe simulations of the full stochastic Eqs. (6) and (7) performed with a spontaneous Langevin term included, and with population noise first of all taken to be zero. Simulations have been performed using the algorithm described in [17], and with an integration step of 3×10^{-5} in normalized time τ. All results were averaged over 400 realizations. The results of calculations of the mean transient time value $\langle T_{tr} \rangle$, and its variance $\sigma = (\langle T_{tr}^2 \rangle - \langle T_{tr} \rangle^2)^{1/2}$, as a function of the modulator phase φ are presented in Figs. 3(a)–3(d) by points and dashed lines, respectively. As can be seen from these figures, the effect of spontaneous noise on the process of targeting the unstable T-periodic orbit is twofold. First, as might be anticipated, the random Langevin term makes phase switchings possible even at some ''detuning'' from the exact targeting values of the modulator phase, and, on the other hand, it diverts a trajectory from a targeting path when accurately tuning to these phases, thus leading to smearing of the sharp targeting peaks in the $\langle T_{tr} \rangle$ versus φ dependencies. In fact, rare events of noise-induced switchings between the antiphased $2T$-periodic attractors are observed even in quiet regimes, i.e., far enough from the targeting phases.

The second visible effect of spontaneous noise is a more pronounced suppression of the middle targeting peak, which is explained by nature of this peak which arises as a consequence of the separatrix folding and tendings to merge with the third peak. Figure 3(d), taken at a smaller modulation frequency ω, demonstrates this nearly degenerate case more explicitly: here the same dependences $\langle T_{tr} \rangle$ versus φ calculated with noise consists only of two peaks. It should be noted, that in patterns with an odd total number of peaks (nondegenerate case) the $2T$-periodic regimes in the different valleys between targeting peaks differ in phase by π. This implies that when one of the peaks disappears dynamically or is smeared out statistically, frequent up and down π phase changes may be induced. The latter is consistent with the recently reported [18] experimental observations of random phase switchings between different 2-periodic regimes in a CO_2 laser with loss modulation. In general, it seems that the first (left-hand-side) peak, which originates in the basic transversal crossing the separatrix by the initial point, is most robust to the influence of noise: it supports the same phase maximum as in the deterministic limit, and has quite a smooth shape under conditions of statistical averaging (400 trajectories). Its position in the phase interval $[0; 2\pi]$ also scales with the noise strength in good agreement with the linear law in Fig. 4. The scaling of the two right-hand-sided peaks is not as good, thus implying that for them nonlinear effects are more important.

The corresponding variance of the mean transient time $\sigma = (\langle T_{tr}^2 \rangle - \langle T_{tr} \rangle^2)^{1/2}$ is also shown at the bottom of Figs. 3(a)–3(d). It can be seen that the variance is dramatically increased in the domain of peak crowding, in fact by more than one order of magnitude. Obviously, the reason is a large dispersion of possible relaxation times near the targeting val-

ues of the modulator phase, therefore the maximal variance values correlated with targeting phases. The variances calculated with different criteria of reaching the final regime, as has been discussed above, are shown at the very bottom of Fig. 3. They practically coincide with each other thus indicating that the coarsening of the criteria is analogous to a purely deterministic rescaling of transient time.

The universality of dependencies obtained at different noise strengths appears to be more interesting. The superimposed results of both $\langle T_{tr} \rangle$ versus φ and σ versus φ nearly coincide, despite having noise strengths which differ by several orders of magnitude [the calculations in Figs. 3(c)–3(a) are given for $\beta = 10^{-6}$, 10^{-8}, and 10^{-10}, respectively]. This means that to first approximation the statistics of such a nonlinear stage of laser turn-on do not depend on the noise levels, so that even in the limit $\beta \to 0$ the same spread of targeting peaks might be anticipated. The qualitative explanation of this effect is rooted again in the self-similarity of the heteroclinic structure discussed in Sec. III A. As the spontaneous background which initiates laser action tends to zero, the dispersion of the initial conditions correspondingly decreases, but due to the infinitely dense heteroclinic structure the reduced noisy initial cloud effectively covers the same number of the heteroclinic crossings, and essentially the same statistics are obtained. Similarly, negligibly small noise may cause a macroscopic effect of π phase slipping of the final $2T$-periodic attractor, while the transient trajectory approaches the unstable T-periodic state in the second region of the heteroclinic structure [near the thick line in Fig. 2(a)].

Highest passage time distributions. Following the pioneering work by Arecchi and Politi [19] the method of the first passage time (FPT), has been widely used in studies of laser switch-on statistics. In a laser the passage time is defined as the time needed to build up intensity to a prefixed level starting from the instant of laser turn-on, and may be identified with the lifetime of the initial unstable state. The width of the FPT distribution gives a value of jitter in a laser, which is of paramount importance in optical communications applications. However, the FPT technique describes the very first linear regime of laser amplification. Therefore, in this paper we focus on the highest passage time (HPT) distributions to explore the nonlinear regime of the noisy laser. The highest passage time may be defined similarly as the time needed for a laser to reach the preassigned value of intensity for a second, third time, and so on. The only additional condition is to attach this definition to a leading edge of the pulses. Such an approach is especially useful in the case of modulated lasers. In the case of simple relaxation oscillations (the prefixed value then is just the steady state) the HPT distributions are progressively broadened functions reflecting the fact of rising multiple nonlocked random responses at the relaxation frequency as the intensity approaches the steady state. In a nonbifurcating laser the situation is better: external modulation locks the relaxation oscillations in stationary modulation regimes, and therefore the width of the high passage time distribution is quite narrow. However, if the modulation frequency does not match the relaxation one, the process of lock-in takes some time, resulting in large fluctuations in the intermediate transient. In particular, in such a setting, we observed the second pulse jitter to be significantly larger than that of the first giant pulse.
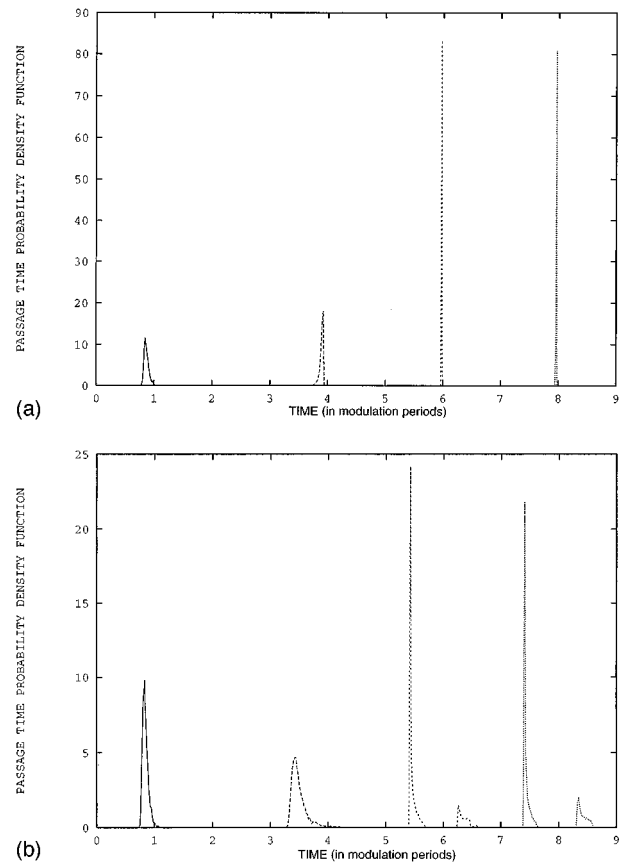
FIG. 5. First four passage time distribution functions for the modulator phase $0.6 \times 2\pi$ (a) and $0.08 \times 2\pi$ (b). All other parameters are as in Fig. 3(a).

In Figs. 5(a) and 5(b), we present the first four passage time distribution functions for a "silent" phase of Q switching, i.e., far enough from the region of the targeting peaks crowding ($\varphi/2\pi = 0.6$) and for a "noisy" phase taken at the left slope of the first targeting peak in Fig. 3(a) ($\varphi/2\pi = 0.08$), respectively. The prefixed level has been chosen to be $u = 1.63$. In the former case the distributions behave classically: the most severe fluctuations take place at the very beginning of transients, producing large jitter for the first pulse, then the width of distributions are quickly narrowed, signaling the decay of anomalous transient fluctuations. The corresponding intensity traces in time are shown in Fig. 6(a). Conversely, in the latter case [Fig. 5(b)] the highest passage time distribution become progressively double-peak shaped. The typical time traces of transients for such double-peak HPT arrangement is depicted in Fig. 6(b), and clearly shows that the origin of the double-peak shape of the third passage time is the trajectory's phase slipping by π near the separatrix, whereas the asymmetrical broadening of the second passage time distribution originates in the partial phase slipping at the fast manifold of the attracting $2T$-periodic regime [cf. dips in the deterministic top dependence $\langle T_{tr} \rangle$ versus φ in Fig. 3(a)]. The important property of the HPT distributions is the fact that all of them, starting from the third one, are symmetrical in the exact targeting phases, and invert the kind of symmetry upon crossing that value of the phase, while the FPT distribution remains nearly intact. The nature of the asymmetrical broadening of the sec-
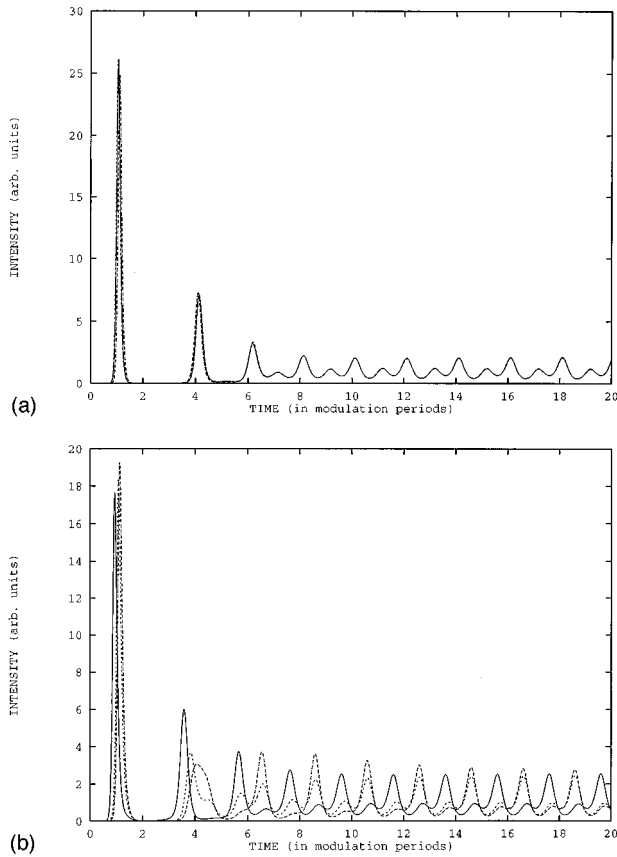
FIG. 6. Representative transient laser intensities vs time corresponding to Figs. 5(a) and 5(b).

ond passage time distribution function is defined by the fast manifolds located between first and second targeting peaks, so it changes its symmetry and location of maximum [compare Figs. 5(a) and 5(b)] at the midpoint between these peaks, or more precisely, between the two dips seen in Fig. 3(a) (solid line). Thus the symmetry and double structure of the HPT distributions reflects the structure of the Poincaré section of the underlying dynamical system. As a final point, we also observe a nearly linear (and opposite in sign) dependence of the maximal intensities of the first pulses on the corresponding first passage time. This is simply attributed to the fact that during the first passage time the cavity losses rise as $\cos(0.6 \times 2\pi + \omega\tau)$ in Fig. 6(a), and fall as $\cos(0.08 \times 2\pi + \omega\tau)$ in Fig. 6(b), so, correspondingly, the later the giant pulse is built up the worse (the better) is the relation between losses and gain.

Influence of pump noise. We have also performed a few preliminary simulations with the pump Langevin noise included, and describe the results for the sake of completeness. In a real experimental situation the spontaneous emission contribution to the population noise is normally negligible in comparison with other noise sources, so we adopt here the data of Giofini *et al.* [20], yielding the estimate for the noise strength term $\delta = 2.5 \times 10^{-5}$. The spontaneous noise strength has been chosen to be $\beta = 10^{-8}$ and $\eta = 2$ (two-level model). In spite of such a huge different it has been found that the population noise alone leads only to a very slight smearing of the targeting peaks, and being taken in combination with the spontaneous noise emission does not produce any statis-

tically meaningful changes of the targeting peaks widths and heights. The explanation for this is that population noise acts mainly along the stable manifold of a laser offset, and any perturbations of this manifold tend to decay, whereas any tiny perturbations along the unstable outset are amplified by approximately $e^{\gamma T} \cong 10^{12}$ times during only one period of modulation. The presence of the heteroclinic structure does not change the situation significantly, at least near regular targeting peaks. Curves 2 and 2′ of Fig. 2 approach the stable manifold of the laser off-state nearly tangently, so the population noise does not cause their crossing. We observe, however, that in special case of degeneracy, when one of the curves 2 or 2′ tangentially touches the outset, the picture inverts. Now the spontaneous noise acts tangentially to the separatrix, but the population noise acts transversally. As a result, the population noise contributes to the broadening of these degenerate peaks significantly. More detailed results will be reported elsewhere [21].

IV. DISCUSSION

The above obtained scaling law and the universality of the turn-on statistics (i.e., $\langle T_{tr} \rangle$ versus φ dependencies) are by no means unique in such studies: it is well known, e.g., that the first passage time in class-A lasers scales logarithmically with the spontaneous emission noise, while its dispersion (jitter) remains independent of the noise strength [4]. But, as has already been mentioned, the first passage time technique is most useful in studies of the very first stage of laser amplification, while in this paper attention is given to a whole range of a transient process in a bifurcating laser where noise effects are also very important. The dynamics characterized here is, moreover, in a strongly nonlinear regime. Such terms as the total transient time, targeting phases, or heteroclinic intersection cannot even be defined in the linear limit. Nonetheless, the scaling law obtained is well described by a linear mapping. Application of the HPT technique proved to provide much more information about turn-on statistics than just using single FPT. The appearance of interesting features in the HP statistics, namely, the double-peak structure of different origin, seems not to have been observed previously. Two-peaked distributions of the FPT distribution reported so far in a single-mode CO_2 laser [20], two-mode dye [22], and semiconductor lasers [23] modulated at the GHz rate, were observed either due to the special initial setting near the threshold value or correlation between two modes or two successive pulses.

The obtained regularities of Q switchings suggest that there is considerable scope for experiments in this field. For instance, from Eqs. (8) and (11) it is seen that the targeting peak location is a linear function of the logarithm of the hold-off ratio k. This latter parameter may be readily tuned experimentally, so that experimental confirmation of the predicted scaling is technically possible. The resolution of such a scheme would be limited by the factor of statistical spreading of the targeting peaks. In this respect the symmetry properties of the highest passage time statistics may be a possible alternative method of measurement of the location of targeting peaks. Further, with the scheme presented, some noticeable aspects of practical relevance might be examines such as the detection of weak injected signals. The HPT distribu-

tions near the targeting peaks are expected to be extremely sensitive to such weak signals, suggesting that previous sensitivity gained on the basis of the FPT may be improved. As far as the targeting itself is concerned in the context of possible application in laser chaos control schemes, the statistical spread of the targeting phases, of course, hinders its efficiency, although it is still possible in the statistical sense, i.e., with repeated trials, or with use of an external signal which normally makes the statistical spread narrower. Due to the strong foldings of the separatrix just above the period-doubling bifurcation, the probability distributions for the highest passage times becomes progressively two peaked shaped, so that the system behaves statistically even with very small driven noise. This explains the recently reported experimental observations of random phase switchings between different 2-periodic regimes in a CO_2 laser with loss modulation [18]. Finally, we wish to emphasize that similar effects also seem to occur under gain switching, e.g., in laser diodes [24].

V. CONCLUSION

We investigated the influence of intrinsic laser noise on recently proposed schemes for targeting laser dynamics to unstable periodic orbits by means of Q switching of class-B lasers. Several interesting features of turn-on statistics in such a nonlinear regime have been found, including scaling of targeting peaks locations with the strength of the spontaneous emission noise, and the universality of the transient time statistics, i.e., their essential independence of the strength of noise and double-peaked structure of the highest passage times distribution functions with their underlying symmetry properties. The noise has been found to cause much more frequent phase switching in comparison with the deterministic case with possible detrimental effects on the use of this particular scheme in chaos control techniques. In practical schemes the statistical spread of the targeting phases may, however, be reduced by injecting an external signal.

[1] F. T. Arecchi, V. Degiorgio, and B. Querzola, Phys. Rev. Lett. **19**, 1168 (1967); F. T. Arecchi and V. Degiorgio, Phys. Rev. A **3**, 1108 (1971); F. T. Arecchi, in *Noise in Nonlinear Dynamical Systems*, edited by F. Moss, L. Lugiato, and W. Schleich (Cambridge University Press, Cambridge, 1990), pp. 263–269.

[2] P. Spano, A. D'Ottavi, A. Mecozzi, and B. Daino, Appl. Phys. Lett. **52**, 2203 (1988).

[3] L. N. Langley and K. A. Shore, Opt. Lett. **18**, 1432 (1993).

[4] M. San Miguel, in *Laser Noise*, edited by R. Roy (SPIE, Boston, 1990), p. 272; A. Valle, M. A. Rodriguez, and C. R. Mirasso, Opt. Lett. **17**, 1523 (1992); S. Balle, P. Colet, and M. San Miguel, Phys. Rev. A **43**, 498 (1991).

[5] N. B. Abraham, P. Mandel, and L. M. Narducci, *Progress in Optics XXXV*, edited by E. Wolf (Elseview, Amsterdam, 1988), p. 1.

[6] L. A. Kotomtseva, A. V. Naumenko, A. M. Samson, and S. I. Turovets (unpublished).

[7] F. T. Arecchi, G. L. Lippi, G. P. Puccioni, and J. R. Tredicce, Opt. Commun. **51**, 3081 (1985).

[8] A. M. Samson, S. I. Turovets, V. N. Chizhevsky, and V. V. Churakov, Zh. Éksp. Teor. Fiz. **101**, 1177 (1992) [Sov. Phys. JETP **74**, 628 (1992)]; V. N. Chizhevsky and S. I. Turovets, Phys. Rev. A **50**, 1840 (1994).

[9] A. Siegman, *Lasers* (University Science Books, Mill Valley, CA, 1986).

[10] A. M. Samson and S. I. Turovets, Dok. Akad. Nauk SSSR **31**, 888 (1987).

[11] A. Valle, L. Pesquera, and M. A. Rodriguez, Phys. Rev. A **45**, 5243 (1992).

[12] C. W. Gardiner, *Handbook of Stochastic Methods* (Springer-Verlag, Berlin, 1993).

[13] A. M. Samson, Yu. A. Logvin, and S. I. Turovets, Izv. Vyssh. Uchebn. Zaved. Radiofiz. **33**, 49 (1990).

[14] J. M. T. Thompson and H. B. Stewart, *Nonlinear Dynamics and Chaos* (Wiley, New York, 1986).

[15] E. Ott, C. Greboggi, and J. A. Yorke, Phys. Rev. Lett. **64**, 1196 (1990); R. Roy, T. W. Murphy, T. D. Maier, Z. Gills, and E. R. Hunt, *ibid.* **68**, 1259 (1992).

[16] S. I. Turovets and K. A. Shore (unpublished).

[17] J. M. Sancho, M. San Miguel, S. L. Katz, and J. D. Gunton, Phys. Rev. A **26**, 1589 (1982).

[18] P. Glorieux, C. Lepers, R. Corbalan, J. Cortit, and A. N. Pisarchik, Opt. Commun. **118**, 309 (1995).

[19] F. T. Arecchi and A. Politi, Phys. Rev. Lett. **45**, 1219 (1980).

[20] M. Giofini, R. Meucci, P. Wang, and F. T. Arecchi, Europhys. Lett. **21**, 735 (1993).

[21] A. Valle, S. I. Turovets, and K. A. Shore (unpublished).

[22] A. W. Yu, G. P. Agrawal, and R. Roy, J. Stat. Phys. **54**, 1223 (1989).

[23] T. M. Shen, IEEE J. Lightwave Technol. **7**, 1394 (1989).

[24] L. N. Langley, S. I. Turovets, and K. A. Shore, Opt. Lett. **20**, 725 (1995); IEE Proc. Optoelectron. **142**, 157 (1995).